Reaction Mechanism Investigation Using Vibrational Mode Analysis for the Multichannel Reaction of $CH_3O + CO$

ZHOU, Zheng-Yu*,[a,b](周正宇) CHENG, Xue-Li[a](程学礼) GUO, Li[a](郭丽)

[a] *Department of Chemistry, Qufu Normal University, Qufu, Shandong 273165, China*

[b] *State Key Laboratory Crystal Materials, Shandong University, Jinan, Shandong 250100, China*

On the basis of the computed results got by the Gaussian 94 package at B3LYP/6-311++G level, the reaction mechanism of CH_3O radical with CO has been investigated thoroughly via the vibrational model analysis. And the relationships among the reactants, eight transition states, four intermediates and various products involved this multichannel reaction are elucidated. The vibrational mode analysis shows that the reaction mechanism is reliable.**

Keywords multichannel reaction, vibrational mode analysis, B3LYP, CH_3O

Introduction

The methoxy radical (CH_3O) is an important intermediate in the photochemical oxidation of hydrocarbons in the atmosphere,[1-3] and plays a significant role in transforming nitric oxide to nitrogen dioxide.[4] Similarly, the reaction mechanisms of hydroxyl and carbon monoxide[5,6] and of isomerization reaction for chlorofluoromethanol in gas phase[7] were investigated extensively. The reaction of $CH_3O + CO$ is also an important process in methane combustion. So the reaction mechanism of the CH_3O radical in atmospheric gases attracts our interests. Former studies and the work of Wang and his team[8] have carried out the multichannel RRKM calculations for the total and individual rate constants of various channels over a wide range of temperature and pressures using *ab initio* data. In this study, we will use the vibrational modes analysis to elucidate the reaction mechanism.

Computation method

The optimizations of the reactants, intermediates (IM) transition states (TS) and products are performed with the Gaussian 94 programs[9] at the B3LYP/6-311++G** level. The popular hybrid density functional B3LYP method, namely Becke's three-parameter nonlocal exchange functional[10] with the nonlocal correlation functional of Lee, Yang and Parr,[11] is used throughout the study. Subsequently, connections of the transition states and products are confirmed by intrinsic reaction coordinate (IRC) calculations.[12] The reaction conditions are 298.15 K and 1.0000 atmospheric pressure. All the stationary points have been identified for the minimum (number of imaginary frequency, NIMAG = 0) or the transition state (NIMAG = 1) which are confirmed by the IRC calculations.

Results and discussion

The geometries of reactants, intermediates, transition states and products involved in the $CH_3O + CO$ reaction are fully optimized. The schematic potential energy profile was drawn out and depicted in Fig. 1.

Vibrational mode analysis for the reactions of CH_3O *with* CO

There are two reaction channels involved in the

* E-mail: zhengyu@qfnu.edu.cn

Received December 14, 2001; revised March 10, 2002; accepted April 19, 2002.

Project supported by the National Natural Science Foundation of China (No. 2967305), the Natural Science Foundation of Shandong Province (No. Y99B01) and the State Key Laboratory Foundation of Crystal Material.

CH_3O with CO reaction, and the optimized configurations and reaction process can be described as Fig. 2. The vibrational frequencies and their vibrational mode assignment are listed in Table 1.

The C atom of CO can add to the O atom of reactant CH_3O via transition state **TS1**, forming **IM1**. For **TS1**, three C-O-C-O modes and the C(2)-O(1) stretch mode at i331 cm^{-1} denote the formation of the C(2)—O(1) bond. Again, the imaginary frequency is relative to the forming bond. Moreover, the relatively low imaginary frequency may indicate a relatively low energy barrier, so it is not surprising that the internal energy of **TS1** is only 20.63 kJ/mol. There are three C-O stretch modes: one is the imaginary frequency; the other two are C(1)—O

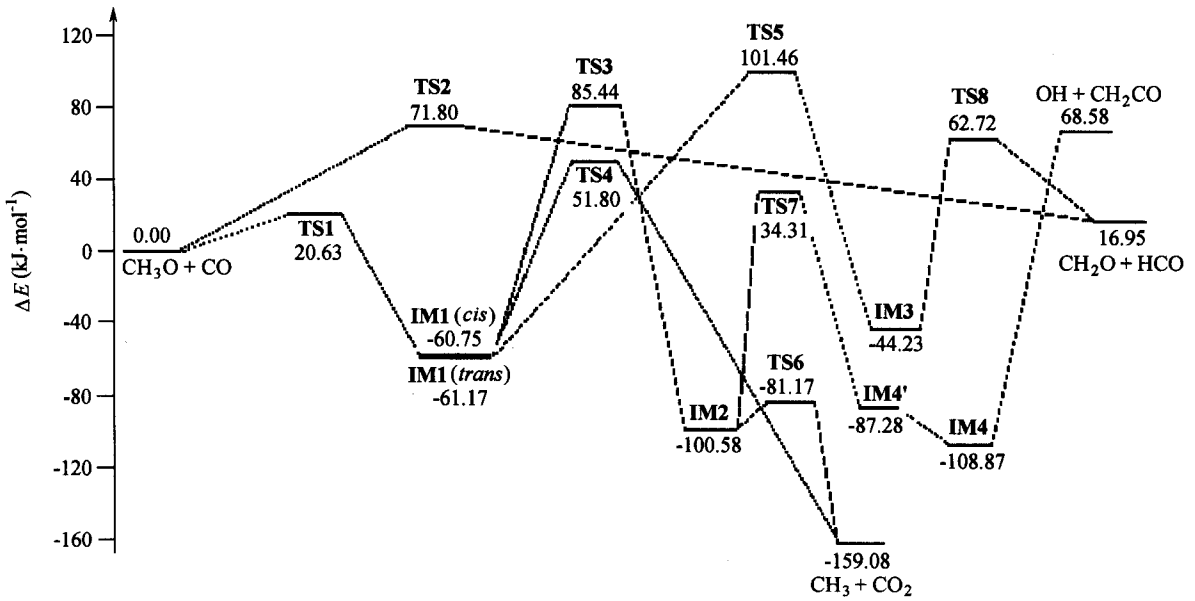

Fig. 1 Energetic profile (in kJ/mol) of the potential energy surface for the CH_3O + CO reaction at B3LYP/6-311 + +G * * level.

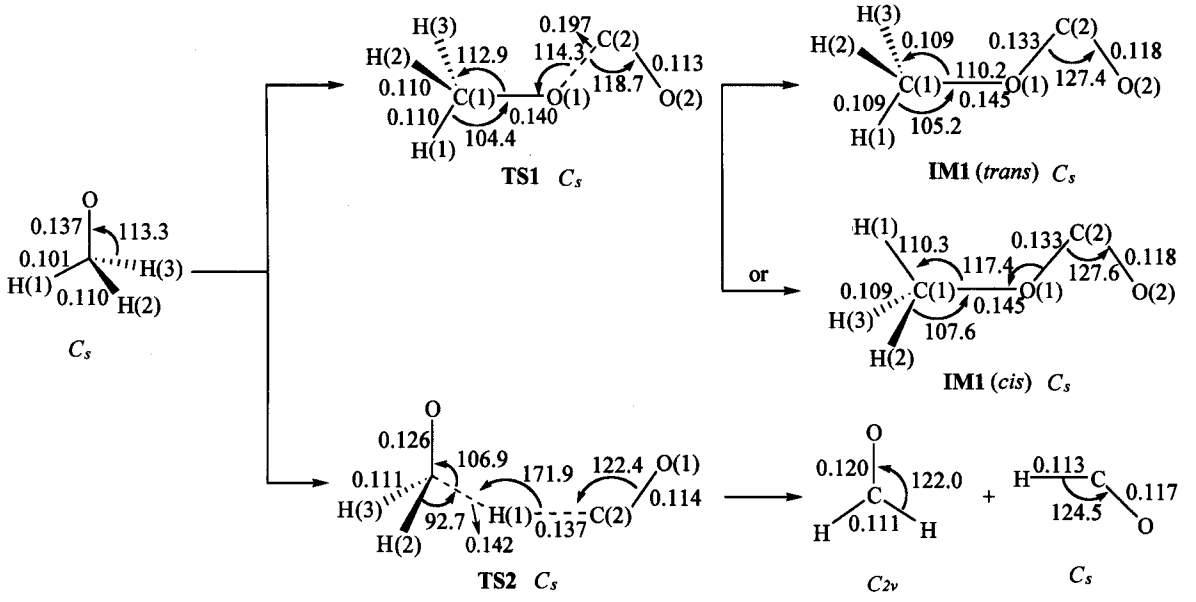

Fig. 2 B3LYP/6-311 + +G * * optimized geometrical parameters for various species involved in the CH_3O + CO reaction. Bond lengths are in nm and bond angles in degrees. Numbers besides the H atoms are sequence numbers to distinguish them.

Table 1 Vibrational frequencies and vibrational mode assignment for **TS1**, **TS2**, **IM1** (*trans*) and **IM1** (*cis*)

Species	Freq.	Freq. assignment	Species	Freq.	Freq. assignment
TS1	i311	C(2)-O(1) stretch	**IM1** (*trans*)	70	O-CH_3 twist
	100	C-O-C-O twist		215	C-O-C-O twist
	157	O-CH_3 twist		317	C-O-C-O rock in plane
	202	C-O-C-O rock in plane		615	C-O-C-O asymmetric stretch
	330	C-O-C-O bend in plane		981	C-O-C bend in plane
	991	C(1)-O(1) stretch		1111	C-O-C asymmetric stretch
	1118	CH_3 rock in plane		1169	H(2)-C-H(3) twist
	1147	H(2)-C-H(3) twist		1215	CH_3 rock in plane
	1412	CH_3 bend in plane		1473	CH_3 bend in plane
	1413	CH_3 twist		1491	CH_3 twist
	1507	H(2)-C-H(3) bend in plane		1497	H(2)-C-H(3) bend in plane
	2140	C(2)-O(2) stretch		1872	C(2)-O(2) stretch
	2966	CH_3 symmetric stretch		3053	H(2)-C-H(3) symmetric stretch
	3027	CH_3 asymmetric stretch		3134	H(2)-C-H(3) asymmetric stretch
	3060	H(2)-C-H(3) asymmetric stretch		3165	C-H(1) stretch
IM1 (*cis*)	57	O-CH_3 twist	**TS2**	i1711	C(1)-H(1) stretch
	231	C-O-C-O twist		45	O(1)-C(1)-H(1) twist
	328	C-O-C-O rock in plane		91	O-CHC-O rock in plane
	618	C-O-C-O asymmetric stretch		355	C(1)-O(2) rock in plane
	975	C-O-C bend in plane		380	CH_3 twist
	1107	C-O-C rock in plane		442	C-H-C symmetric stretch
	1173	H(2)-C-H(3) twist		883	C(1)-H(1) twist
	1232	H1-C-O-C rock in plane		1029	C(1)-H(1) rock in plane
	1468	CH_3 bend in plane		1216	H(2)-C-H(3) twist
	1487	CH_3 twist		1272	CH_3 bend in plane
	1503	H(2)-C-H(3) bend in plane		1456	H(2)-C-H(3) bend in plane
	1867	C(2)-O(2) stretch		1585	C(1)-O(2) stretch
	3055	CH_3 symmetric stretch		2084	C(2)-O(1) stretch
	3144	H(2)-C-H(3) asymmetric stretch		2859	H(2)-C-H(3) symmetric stretch
	3145	CH_3 asymmetric stretch		2924	H(2)-C-H(3) asymmetric stretch

(1) (991 cm^{-1}) and C(2)—O(2) (2140 cm^{-1}). Different frequencies should attribute to their different bond lengths (0.197 nm, 0.140 nm and 0.113 nm, respectively).

Intermediate **IM1** has two isomers, the *trans*- and *cis*-configuration. The emergence of the C-O-C vibrational modes implies that a stable C(2)—O(1) bond forms. Because their vibrational frequencies and vibrational modes only differ from each other slightly, from Table 1 it can be seen that the two species should have close potential energies. Fig. 1 shows that the energy of the *cis*-configuration is larger than those of the *trans*-configuration near only 0.42 kJ/mol. For the *trans*-isomer, a C-O-C bend in plane mode emerges at 1107 cm^{-1}, instead of a C-O-C stretch mode (1111 cm^{-1}) in the *cis*-isomer.

CO can abstract a hydrogen atom from CH_3O to produce CH_2O and HCO via **TS2**. The C-H(1) stretch mode at 2889 cm^{-1} of CH_3O is decreased to C(1)-H(1) stretch mode at i1711 cm^{-1} in **TS2**, which is the imaginary frequency. Fig. 1 testifies that the internal energy of **TS2** is equal to 73.68 kJ/mol. The O(1)-C(2)-H(1) twist mode (45 cm^{-1}), the O-CHC-O rock in plane mode (91 cm^{-1}) and the C-H-C symmetric mode (442 cm^{-1}) show that the migrating hydrogen atom has already added to the carbon atom of CO; at the same time, the C(1)-H(1) twist and the C(1)-H(1) rock in plane mode together with the imaginary frequency denote that this

atom has not completely immigrated from CH_3O radical.

Vibrational mode analysis for reaction channels of **IM1**

The two configurations of **IM1** involve three reaction channels, which can be described in Fig. 3. The vibrational frequencies and vibrational mode assignment of **TS3**, **IM2**, **TS4** and **TS5** are listed in Table 2, but those of **IM3** are shown in Table 3.

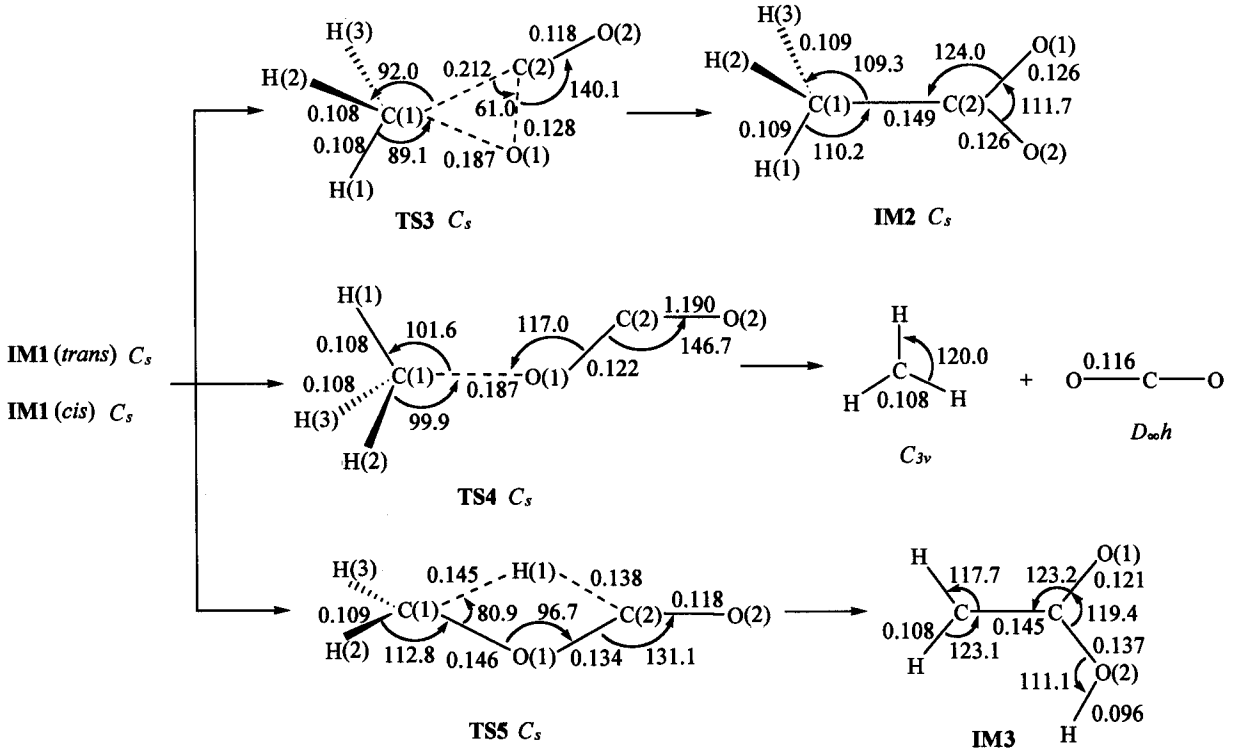

Fig. 3 Optimized configurations involved the reaction of **IM1**.

Table 2 Vibrational frequencies and vibrational mode assignment of **TS3**, **IM2**, **TS4** and **TS5**

Species	Freq.	Freq. assignment	Species	Freq.	Freq. assignment
TS3	i971	C(2)-C(1)-O(1) bend in plane	**IM2**	33	CH_3 twist
	59	C-CH_3 twist		397	C-CO_2 twist
	233	O-C-O rock out of plane		553	C-C twist
	283	C-C stretch		572	CO_2 bend in plane
	657	O-C-O bend in plane		900	C-CO_2 bend in plane
	848	H(2)-C-H(3) twist		988	CH_3 rock in plane
	893	C-H(1) rock in plane		1057	C-CH_2 twist
	1147	C-CH_2 rock in plane		1139	CO_2 asymmetric stretch
	1249	CH_3 bend in plane		1388	CH_3 bend in plane
	1438	H(2)-C-H(3) bend in plane		1457	H(2)-C-H(3) rock out of plane
	1449	CH_3 twist		1585	C-H(1) twist
	1915	C(2)-O(2) stretch		1466	C-CO_2 asymmetric stretch
	3094	CH_3 symmetric stretch		3045	CH_3 symmetric stretch
	3222	CH_3 asymmetric stretch		3116	H(2)-C-H(3) asymmetric stretch
	3257	H(2)-C-H(3) asymmetric stretch		3135	CH_3 asymmetric stretch

Continued

Species	Freq.	Freq. assignment	Species	Freq.	Freq. assignment
TS4	i1338	C-O-C bend in plane	**TS5**	i2047	C-H(1) rock in plane
	35	CH_3 twist		210	C-O(2) twist
	246	C-O-C-O rock in plane		480	C-O-C-O rock in plane
	350	C(2)-O(2) twist		496	C-CH_2 twist
	647	C-O-C rock in plane		719	C-O-C-O bend in plane
	746	H(2)-C-H(3) twist		902	C(1)-O(1) rock in plane
	816	C-H(1) rock in plane		1004	C(1)-O(1) stretch
	983	O-C-O symmetric stretch		1127	H(2)-C-H(3) twist
	1141	CH_3 bend in plane		1166	C(2)-O(2) stretch
	1426	C-H(1) twist		1169	C-H(1) twist
	1432	H(2)-C-H(3) rock out of plane		1462	H(2)-C-H(3) bend in plane
	2006	C(2)-O(2) stretch		1888	O(2)-C(2)-H(1) rock in plane
	3087	CH_3 symmetric stretch		1920	O(2)-C(2)-H(1) bend in plane
	3256	CH_3 asymmetric stretch		3102	H(2)-C-H(3) symmetric stretch
	3268	H(2)-C-H(3) asymmetric stretch		3224	H(2)-C-H(3) asymmetric stretch

The oxygen atom of *trans*- or *cis*-**IM1** can be shifted to the carbon atom of CO via a three-atom-ring transition state **TS3**, leading to **IM2**. The only imaginary frequency (i971 cm^{-1}) of **TS3** is assigned to the C(2)-C(1)-O(1) bend in plane mode. The emergences of O-C-O rock out of plane mode and bend in plane mode prove the formation of the C(2)—O(1) bond. The C-C stretch mode appears at the fingerprint region of 283 cm^{-1} instead of at the character region, denoting the C—C is prolonged. Fig. 1 shows the C—C bond is 0.212 nm by length. In **IM2**, the C-CO_2 twist (397 cm^{-1}) mode and bend in plane mode (900 cm^{-1}) show that the immigrating oxygen atom has completely added to the C(2) atom.

The second reaction channel of **IM1** is the O-elimination process via **TS4**, leading to CH_3 + CO. The imaginary frequency is the C-O-C bend in plane mode (i1338 cm^{-1}) and the breaking C(1)—O(1) bond is prolonged to 0.187 nm. For **TS4**, the C-O-C-O rock in plane mode is reduced to 246 cm^{-1}, at the same time the C-O-C rock in plane mode is decreased to 647 cm^{-1}, which show that the C(1)—O(1) bond is weakened. But the appearance of O-C-O symmetric stretch (983 cm^{-1}) shows the C(2)—O(1) bond is enhanced. With the C-H is being shortened, from Fig. 1 and Table 3 it can be observed that the modes of CH_3 stretch and the CH_2 stretch are reinforced.

A hydrogen atom in the CH_3 group of **IM1** can migrate to C(2) atom via a four-atom-ring **TS5** to form **IM3**. For **TS5**, the imaginary frequency belongs to the C-H(1) rock in plane mode. The O(2)-C(2)-H(1) bend in plane mode (1462 cm^{-1}) and its rock in plane mode (1888 cm^{-1}) may be the symbols of the H(1) atom shifting to the terminal C(2) atom. Furthermore, all CH_3 vibrational modes disappear because the C(1)—H(1) bond is elongated to 0.138 nm. In **IM3**, the C(1)—H(1) bond ruptures entirely, and the C(2)—H(1) bond forms, so all C(1)-H(1) vibrational modes of **IM1** vanishes, but new C(1)-H(1) twist mode (1015 cm^{-1}), rock in plane mode (1400 cm^{-1}) and stretch mode (2983 cm^{-1}) are emerged.

Reaction channel of **IM2** *and* **IM4**

The two reaction pathways of **IM2** are depicted in Fig. 4. The frequencies and vibrational mode assignments of **TS6**, **TS7**, **IM4'** and **IM4** are shown in Table 4.

The first reaction pathway of **IM2** is the C-C rupture process via transition state **TS6**. The solitary imaginary frequency belongs to the O-C-O rock in plane mode (i414 cm^{-1}) involved the migrating CO_2 group. Because the C—C bond is elongated to 0.157 nm, the C-C stretch mode (642 cm^{-1}) appears at the finger print region. There are two C-O stretch modes, namely C-O(2) (935 cm^{-1}) and C-O(1) (1763 cm^{-1}) stretch mode, which can be due to their different bond lengths. Fig. 4 shows the bond lengths are 0.130 nm and 0.120 nm, respectively.

Table 3 Vibrational frequencies and vibrational mode assignments of **IM3** and **TS8**

Species	Freq.	Freq. assignment	Species	Freq.	Freq. assignment
IM3	150	C-O-C-O twist	**TS8**	i533	C(1)-O(2) stretch
	243	CH_2 twist		90	C-O-C-O twist
	281	CH_2 rock out of plane		226	O-C-H(2) rock out of plane
	359	C-O-C-O rock in plane		283	C-H(3) rock out of plane
	643	C-O-C-O bend in plane		422	C-O-C-O bend in plane
	1015	C(1)-H(1) twist		727	C-H(1) twist
	1019	C(1)-O(2) stretch		969	CH_2 rock out of plane
	1167	H(2)-C-O asymmetric stretch		1081	C-H(1) rock in plane
	1244	H(3)-C-O bend in plane		1224	CH_2 twist
	1400	C(1)-H(1) rock in plane		1417	C(2)-O(2) stretch
	1466	CH_2 bend in plane		1572	C(2)-O(2) bend in plane
	1841	C(1)-O(1) stretch		1903	C-O(1) stretch
	2983	C(1)-H(1) stretch		2760	C-H(1) stretch
	3151	CH_2 symmetric stretch		2981	CH_2 symmetric stretch
	3315	CH_2 asymmetric stretch		3076	CH_2 asymmetric stretch

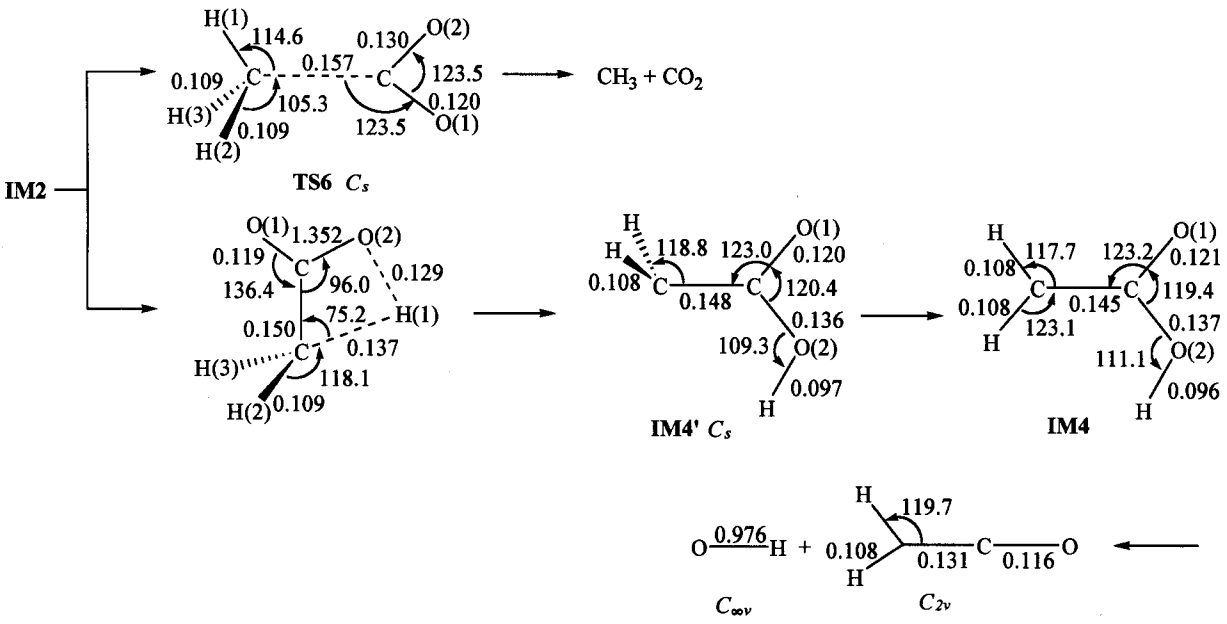

Fig. 4 Optimized structures of reaction channels of **IM2** and **IM4**.

Table 4 Vibrational frequencies and vibrational mode assignment of **TS6**, **TS7**, **IM4'** and **IM4**

Species	Freq.	Freq. assignment	Species	Freq.	Freq. assignment
TS6	i414	O-C-O rock in plane	**TS7**	i2013	C-H(1) rock in plane
	105	CH_3 twist		404	CH_3 twist
	395	C-CO_2 bend in plane		501	C-CO_2 rock in plane
	601	C-CH_2 twist		542	C-CH_2 twist
	642	C-C stretch		606	C-CO_2 bend in plane
	935	C-O(2) symmetric stretch		927	C-C-O2 bend in plane
	993	C-CH_3 twist		992	H(2)-C-H(3) rock out of plane

Continued

Species	Freq.	Freq. assignment	Species	Freq.	Freq. assignment
	1105	C-C-H(1) bend in plane		1036	H(2)-C-H(3) twist
	1350	CH_3 bend in plane		1094	C-H(1) twist
	1432	H(2)-C-H(3) bend in plane		1150	C-C-O(2) asymmetric stretch
	1474	C-H(1) twist		1397	H(2)-C-H(3) bend in plane
	1763	C-O(1) stretch		1778	C-O(1) stretch
	3048	CH_3 symmetric stretch		1966	C-H(1) rock in plane
	3144	H(2)-C-H(3) asymmetric stretch		3110	H(2)-C-H(3) symmetric stretch
	3153	CH_3 asymmetric stretch		3218	H(2)-C-H(3) asymmetric stretch
IM4'	i306	CH_2 twist	**IM4**	223	CH_2 twist
	370	C-CH_2 rock in plane		416	O-H twist
	510	C-O-H twist		443	CH_2 rock in plane
	568	C-C-O(2) bend in plane		599	CO_2 bend in plane
	586	C-CH_2 twist		607	C-CH_2 twist
	625	C-CO_2 bend in plane		742	C-CH_2 rock out of plane
	889	C-CO_2 symmetric stretch		896	C-CO_2 asymmetric stretch
	1029	C-CH_2 twist		985	C-H(1) rock in plane
	1152	C-O-H rock in plane		1184	H-O rock in plane
	1301	C-O-H bend in plane		1307	H-O-C bend in plane
	1414	CH_2 bend in plane		1466	CH_2 bend in plane
	1810	C-O(1) stretch		1695	C-O(1) stretch
	3145	CH_2 symmetric stretch		3146	CH_2 symmetric stretch
	3256	CH_2 asymmetric stretch		3269	CH_2 asymmetric stretch
	3780	O-H stretch		3822	O-H stretch

Atom H(1) of the methyl group can add to the O atom via a four-atom-ring **TS7**. In **TS7**, the C-H(1) stretch mode at i2013 cm^{-1} is the imaginary frequency. The CO_2 asymmetric stretch (1139 cm^{-1}) and the C-CO_2 asymmetric stretch (1585 cm^{-1}) of **IM2** disappear, but a C-C-O(2) asymmetric stretch at 1150 cm^{-1} emerges in **TS7**. This may be attributed to the formation of the ring reducing their activity. Except for the CH_3 twist mode (404 cm^{-1}), the other CH_3 vibrational modes also varnish because the C—H(1) bond is pronged to 0.137 nm and shifting to the O(2) atom.

The product of this channel is **IM4'**. The C-O-H twist mode (510 cm^{-1}), rock in plane mode (1152 cm^{-1}), bend in plane mode (1301 cm^{-1}) and O-H stretch mode (3780 cm^{-1}) show that the migrating hydrogen atom has added to the terminal oxygen atom totally. In addition, the CH_3 twist mode of **TS7** varnishes. It is surprising that this species has an imaginary frequency (i306 cm^{-1}) that belongs to CH_2 twist mode. So it is a highly activated intermediate and should be unstable. From Fig. 1, it can be seen that two hydrogen atoms are out of the molecular plane. Subsequently this rich-energy species is transited to **IM4** through a non-barrier process. **IM2** has a planar configuration, and the imaginary frequency of **IM4'** is increased to 223 cm^{-1}. Compared to **IM4'**, the internal energy of **IM4** is decreased by 21.59 kJ/mol. Fig. 4 shows that the C—O(2) (0.137 nm) is longer than normal C—O single bond, and it can decompose directly without a transition state to OH and CH_2CO.

Vibrational mode analysis for the reaction channel of **IM3**

Intermediate **IM3** can produce CH_2O + HCO via **TS8**, as shown in Fig. 5. The C(1)—O(2) bond is lengthened by 0.056 nm, and its stretch vibrational mode is decreased by 1552 cm^{-1} becoming the imaginary frequency. The C—O(1) bond is shorted by 0.002 nm, at the same time the frequency of its stretch mode is increased by 62 cm^{-1}. Because the C—H(1) bond in prolonged by 0.0014 nm, the C-H(1) twist mode, rock in plane mode and the stretch mode are reduced by 288, 319 and 223 cm^{-1}, respectively. There is a C-H(3)

rock out of plane mode (283 cm^{-1}), which shows that the C—H(2) and C—H(3) bond do not equal to each other. In fact, the C—H(3) bond is slightly longer than the C—H(2) bond by 0.0002 nm.

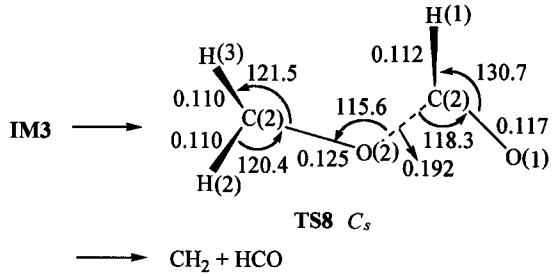

Fig. 5 Optimized structures involved in the reaction channel of **IM3**.

Conclusion

All species involved in the multichannel reaction of the CH_3O with CO has been optimized by utilizing Gaussian 94 procedure package at B3LYP/6-311 + + G * * level. The potential energy surface is drawn out for this reaction. The vibrational mode analysis is used to elucidate the relationships of the transition states, intermediate and the products. From Fig. 1 we can see that CH_3 + CO_2 is the main product because of its lowest internal energy (- 159.08 kJ/mol), so the main reaction channel involving this system should beThe extensive investigation shows that the reaction mechanism is reliable.

$CH_3 + CO \longrightarrow$ **IM1** (*cis*) or **IM1** (*trans*)

$\longrightarrow$ **TS4** $\longrightarrow CH_3 + CO_2$

$\longrightarrow$ **TS3** $\longrightarrow$ **IM2** $\longrightarrow$ **TS6** $\longrightarrow CH_3 + CO_2$

References

1 Aikin, A. C. *J. Geophys. Res.* **1982**, *87*, 3105.

2 Atkinson, R.; Lloyd, A. C. *J. Phys. Chem. Ref. Data* **1984**, *13*, 315.

3 Perner, D.; Platt, U.; Trainer, M.; Hubler, G.; Drummond, J.; Junkermann, W.; Rudolph, J.; Schubert, B.; Volz, A.; Elhalt, D. H. *J. Atmos. Chem.* **1987**, *5*, 185.

4 Heicklen, H.; Westberg, K.; Cohen, N. *The Conversion of NO to NO_2 in Polluted Atmospheres*, The Pennsylvania State University Center for Air Environment Studies, PA, **1969**.

5 Kudla, K.; Schatz, G. C. *J. Chem. Phys.* **1991**, *95*, 1635.

6 Baulch, D. L.; Cobos, C. J.; Cox, R. A.; Esser, C.; Frank, P.; Just, Th.; Kerr, J. A.; Pilling, M. T.; Troe, J.; Walker, R. W.; Warnatz. J. *J. Phys. Chem. Ref. Data* **1992**, *21*, 411.

7 Wang, S.-K.; Hou, H.; Zhang, Q.-Z.; Kong, Z.-Y.; Wang, B.-S.; Gu, Y.-S. *Acta Chim. Sinica* **2001**, *59*, 502 (in Chinese).

8 Wang, B.-S.; Hou, H.; Gu, Y.-S. *J. Phys. Chem. A* **1999**, *103*, 8021, (references therein).

9 Frisch, M. J.; Trucks, G. W.; Schlegel, H. B.; Gill, P. W. M.; Johnson, B. G.; Robb, M. A.; Cheeseman, J. R.; Keith, T, A.; Petersson, G. A.; Montgomery, J. A.; Raghavachari. K.; Allaham, M. A.; Zakr/ewski, V. G.; Ortiz, J. V.; Foresman, J. B.; Cioslowski, J.; Stefanov, B. B.; Nanayakkara, A.; Challacombe, M.; Peng, C. Y.; Ayala, P. Y.; Chen, W.; Wong, M. W.; Andres, J. L.; Replogle, E. S.; Gomperts, R.; Martin R. L.; Fox, D. J.; Binkley, J. S.; Defrees, D. J.; Baker, J.; Stewart, J. P.; Head-Gordon, M.; Gonzales, C.; Pople, J. A. *Gaussian 94*, Gaussian Inc., Pittsburgh, PA, **1995**.

10 Becke, A. D. *J. Chem. Phys.* **1993**, *98*, 5648.

11 Lee, C.; Yang, W.; Parr, R. G. *Phys. Rev. B* **1988**, *37*, 785.

12 (a) Fukui, K.; Kato, S.; Fujimoto, H. *J. Am. Chem. Soc.* **1975**, *97*, 1.
(b) Ishida, K.; Morokuma, K.; Komornicki, A. *J. Chem. Phys.* **1977**, *66*, 2153.
(c) Gonzalez, Z.; Schlegel, H. B. *J. Phys. Chem.* **1989**, *90*, 2154.

(E0112143 LU, Y. J.; HUANG, W. Q.)